A Validation Study of the Fadhloun-Rakha Car-following Model

Karim Fadhloun[1], Hesham Rakha[1] [a], Amara Loulizi[2] [b] and Jinghui Wang[1]

[1]*Virginia Tech Transportation Institute, Virginia Tech, 3500 Transportation Research Plaza, Blacksburg VA, U.S.A.*
[2]*LR11ES16 Laboratoire de Matériaux, d'Optimisation et d'Environnement pour la Durabilité,*
École Nationale d'Ingénieur de Tunis, Tunis, Tunisia

Keywords: Rakha-Pasumarthy-Adjerid Car-following Model, Car-following Behavior, Vehicle Dynamics.

Abstract: The research presented in this paper investigates and validates the performance of a new car-following model (the Fadhloun-Rakha (FR) model). The FR model incorporates the key components of the Rakha-Pasumarthy-Adjerid (RPA) model in that it uses the same steady-state formulation, respects vehicle dynamics, and uses very similar collision-avoidance strategies to ensure safe following distances between vehicles. The main contributions of the FR model over the RPA model are the following: (1) it explicitly models the driver throttle and brake pedal input; (2) it captures driver variability; (3) it allows for shorter than steady-state following distances when following faster leading vehicles; (4) it offers a much smoother acceleration profiles; and (5) it explicitly captures driver perception and control inaccuracies and errors. In this paper, a naturalistic driving dataset is used to validate the FR model. Furthermore, the model performance is compared to that of five widely used car-following models, namely: the Wiedemann model, the Frietzsche model, the Gipps model, the RPA model and the Intelligent Driver Model (IDM). A comparative analysis between the different model outputs is used to determine the performance of each model in terms of its ability to replicate the empirically observed driver/vehicle behavior. Through quantitative and qualitative evaluations, the proposed FR model is demonstrated to significantly decrease the modeling error when compared to the five aforementioned models and to generate trajectories that are highly consistent with empirically observed driver following behavior.

1 INTRODUCTION

Due to the continuous technological advancement and proliferation of computational tools both at the level of hardware and software, traffic engineering is becoming more and more simulation-oriented. Relying on computerized traffic simulations for planning, urbanization and environmental purposes can be cast as a two-edged activity. On the one hand, microscopic simulation software allow the user to evaluate and estimate the outcomes of different potential scenarios in a fast and cost effective manner and, most importantly, without inducing any bottlenecks or disrupting the flow of vehicles in the real world. On the other hand, it is imperative to not forget that the results returned by traffic simulators are directly correlated to the accuracy and precision of the different models and logics incorporated in them. Subsequently, it is necessary to ensure that

whatever implemented in this type of software, would constitute good descriptors of real traffic conditions and empirical behavior.

A main component of microscopic simulation software is the car-following model. Car-following models (Chandler, Herman et al. 1958, Gazis, Herman et al. 1961, Drew 1968, Fritzsche 1994, Treiber, Hennecke et al. 2000, Jiang, Wu et al. 2001, Newell 2002, Olstam and Tapani 2004) predict the temporal and spatial behavior of a following vehicle when the time-space profile of the leading vehicle is known. The output of car-following models directly impact several other factors and measures of effectiveness (MOE), such as vehicle energy/fuel consumption and emissions.

This paper describes a research effort that aims to validate a new innovative acceleration-based car-following model, which is the Fadhloun-Rakha (FR) model. The methodology and the procedure that led

[a] https://orcid.org/0000-0002-5845-2929
[b] https://orcid.org/0000-0003-1542-0086

to the functional form of the model was described extensively in a previous work by Fadhloun and Rakha (Fadhloun and Rakha 2019). The validation of the proposed model is conducted by comparing its performance against the performance of other car-following models. Gipps (Gipps 1981), Frietzsche (Fritzsche 1994), Wiedemann (Wiedemann 1974, Wiedemann 1992), the IDM model (Treiber, Hennecke et al. 2000) and the RPA model (Rakha 2009) were selected as controls of the proposed model because of their wide use and their implementation in some of the most famous traffic simulators (*AIMSUN* (Barceló 2001), *PARAMICS* (Smith, Duncan et al. 1995), *VISSIM* (PTV-AG 2012) and *INTEGRATION* (Van Aerde and Rakha 2007, Van Aerde and Rakha 2007). The dataset used in the validation procedure is extracted from the naturalistic data of the 100-Car study that was conducted by the Virginia Tech Transportation Institute (Dingus, Klauer et al. 2006).

Concerning the layout, this paper is organized as follows. First, an overview of the Fadhloun-Rakha (FR) model is provided along with the other state-of-the-practice car-following models mentioned above. Subsequently, the dataset used in this study is briefly described and the analysis related to the calibration procedure as well as the validation process of the FR model is presented. Finally, the conclusions of the paper are drawn and insights into future work are provided.

2 BACKGROUND

In this section, a brief description of the logic behind each of the studied models is provided in a chronological order.

2.1 Wiedemann Model

The Wiedemann model (Wiedemann 1974) is a psycho-physical car-following model that is widely known in the traffic engineering community due to its integration in the microscopic multi-modal traffic simulation software *VISSIM* (PTV-AG 2012). The initial formulation of the model (Wiedemann 1974), proposed in 1974, was calibrated mostly based on conceptual ideas rather than real traffic data. As a result, a much-needed recalibration of the model (Wiedemann 1992) was performed in the early-1990s using an instrumented vehicle.

The Wiedemann model framework, as implemented in *VISSIM*, uses five bounding functions in the $\Delta v - \Delta x$ domain —*AX*, *ABX*, *SDX*, *SDV* and

OPDV— to define the thresholds between four traffic regimes — free driving, closing-in, following and emergency. Depending on the traffic regime in which the following vehicle is located, the acceleration is set equal to a predefined specific rate. The mathematical expressions of the five regime thresholds are given in Equations (1-5).

$$AX = L_{n-1} + [AX_{add} + AX_{mult} \times RND1] \tag{1}$$

$$ABX = AX + [BX_{add} + BX_{mult} \times RND1]\sqrt{\min(u_{n-1}, u_n)} \tag{2}$$

$$SDX = AX + [EX_{add} + EX_{mult} \times (NRND - RND2)] \times [BX_{add} + BX_{mult} \times RND1]\sqrt{\min(u_{n-1}, u_n)} \tag{3}$$

$$SDV = \left(\frac{\Delta x - L_{n-1} - AX}{CX}\right)^2 \tag{4}$$

$$OPDV = SDV \times [-OPDV_{add} - OPDV_{mult} \times NRND] \tag{5}$$

Where *RND1*, *RND2*, *RND3*, *RND4* and *NRND* are normally distributed parameters that aim to model the randomness associated with different driving patterns and behaviors, L_{n-1} is the length of the leading vehicle in meters, u_{n-1} is the leading vehicle speed in *(m/s)*, *Δx* is the spacing between the lead and the following vehicles, and *CX* is a model parameter that is assumed to be equal to 40. Finally, the remaining variables, named using the standard format P_{add} or P_{mult}, are the model parameters requiring calibration.

It is noteworthy to mention that the formulations of Equations (1-5) could be further simplified by removing the random driver-dependent parameters for the specific case of this study. In fact, the randomness inducing parameters are of no use when calibrating the model against empirical data of a single driver. With that being said, Equations (1-5) are modified by applying the generic transformation of Equation 6 resulting in a significant reduction of the number of calibration parameters. The resultant set of equations, defined in Equations (7-11), requires the calibration of a total of four parameters.

$$P_{cal} = P_{add} + P_{mult} \times P_{rand} \tag{6}$$

$$AX = L_{n-1} + AX_{cal} \tag{7}$$

$$ABX = AX + BX_{cal}\sqrt{\min(u_{n-1}, u_n)} \tag{8}$$

$$SDX = AX + EX_{cal} \times BX_{cal}\sqrt{\min(u_{n-1}, u_n)} \tag{9}$$

$$SDV = \left(\frac{\Delta x - L_{n-1} - AX}{40}\right)^2 \tag{10}$$

$$OPDV = -SDV \times OPDV_{cal} \tag{11}$$

2.2 Gipps Model

Gipps model (Gipps 1981), developed in the late-1970s and implemented in the traffic simulation software *AIMSUN* (Soria, Elefteriadou et al. 2014), is formulated as a system of differential difference equations. Using a time step Δt that aims to model the reaction time of drivers, the model computes the following vehicle speed u_n at time $t+\Delta t$ as a function of its speed and the leading vehicle speed u_{n-1} at the preceding time step t.

As shown in Equation 12, the speed of the following vehicle is estimated by determining the minimum of two arguments. The first term governs the cases characterized by uncongested traffic and relatively large headways. Under such conditions, the following vehicle speed increases until the free-flow speed of the facility u_f is reached. The model formulation is also inclusive of a condition that ensures that u_f is never exceeded once achieved. The second argument of the model is attained when congestion prevails and speeds are constrained by the behavior of the vehicles ahead of them. Due to the collision avoidance mechanism it implements, the congested regime branch is the one responsible for making the Gipps model collision-free.

$$u_n(t+\Delta t) =$$
$$min \left(\begin{array}{c} u_n(t) + 2.5.A_{max}^{des}.\Delta t \left(1 - \dfrac{u_n(t)}{u_f}\right) \sqrt{0.025 + \dfrac{u_n(t)}{u_f}} \\[2ex] D_{max}^{des}.\Delta t + \sqrt{(D_{max}^{des}.\Delta t)^2 - D_{max}^{des}\left[2(\Delta x - L_{n-1}) - \Delta t.u_n(t) - \dfrac{u_{n-1}^2(t)}{\widehat{D}_{n-1}}\right]} \end{array} \right) \quad (12)$$

Where A_{max}^{des} and D_{max}^{des} are the respective desired maximum acceleration and deceleration of the following vehicle in m/s^2, and $\widehat{D}_{n-1}$ denote the maximum deceleration rate of the leading vehicle in m/s^2. Those three parameters are the ones requiring calibration for Gipps model.

2.3 Frietzsche Model

Frietzsche model (Fritzsche 1994) is a car-following model that shares the same structure as Wiedemann model. In this model, six threshold parameters are used to define five driving regimes. The thresholds are defined for four gap (Δx) values and two differences in speed (Δv) values between the leader and the follower vehicles. The four gap threshold parameters, *AR*, *AS*, *AD*, and *AB* are presented in Equations (13-16); while the two differences in speed thresholds, *PTP* and *PTN*, are given in Equations (17-18). We note that the expression of the acceleration rate a_n associated with the "closing in" regime is given in Equation (19-20).

$$AR = s_{n-1} + T_r \times u_{n-1} \quad (13)$$

$$AS = s_{n-1} + T_s \times u_n \quad (14)$$

$$AD = s_{n-1} + T_d \times u_n \quad (15)$$

$$AB = AR + \frac{\Delta u^2}{\Delta b_m} \quad (16)$$

$$PTP = K_{PTP}(\Delta x - s_{n-1})^2 + f_x \quad (17)$$

$$PTN = -K_{PTN}(\Delta x - s_{n-1})^2 - f_x \quad (18)$$

$$a_n = \frac{u_{n-1}^2 - u_n^2}{2d_c} \quad (19)$$

$$d_c = \Delta x - AR + u_{n-1}.\Delta t \quad (20)$$

Where T_r, T_s, T_D and Δb_m are calibration parameters expressed in seconds. For the remainder of this study, $d_{max,}$ f_x, K_{ptp} and K_{ptn} are set equal to -6 m/s^2, 0.5, 0.002 and 0.001.

2.4 The Intelligent Driver Model

The IDM model (Treiber, Hennecke et al. 2000) is a kinematics-based car-following model that is widely used for the simulation of freeway traffic. It was developed in 2000 by Treiber et al. (Treiber, Hennecke et al. 2000) with the main objective of modeling the longitudinal motion of vehicles as realistically as possible under all traffic situations. The fame of this model is mainly due to its mathematical stability, which results in stable vehicle trajectories and smooth acceleration profiles. The acceleration function of the intelligent driver model (IDM) car-following model is presented in Equations (21-22).

$$a_{n+1}(u_{n+1}, s_{n+1}, \Delta u_{n+1}) =$$
$$a\left(1 - \left(\frac{u_{n+1}}{u_f}\right)^\delta - \left(\frac{s^*(u_{n+1}, \Delta u_{n+1})}{s_{n+1}}\right)^2\right) \quad (21)$$

$$s^*(u_{n+1}, \Delta u_{n+1}) = s_j + u_{n+1}T + \frac{u_{n+1}\Delta u_{n+1}}{2\sqrt{a.b}} \quad (22)$$

Where s^* denotes the steady state spacing, a is the maximum acceleration level, b is the maximum deceleration level, δ is a calibration parameter and T is the desired time headway.

2.5 Rakha-Pasumarthy-Adjerid Model

The RPA model (Rakha 2009) is a car-following model that controls the longitudinal motion of the vehicles in the INTEGRATION traffic simulation software (Van Aerde and Rakha 2007, Van Aerde and Rakha 2007). The model is composed of three main components: the steady-state, the collision avoidance

and the vehicle dynamics models. Having the values of its three components, the RPA model computes the speed of the following vehicle as shown in Equation 23.

$$u_{n+1} = min(u_{n+1}^{VA}, u_{n+1}^{CA}, u_{n+1}^{DYN}) \qquad (23)$$

Here u_{n+1}^{VA}, u_{n+1}^{CA} and u_{n+1}^{DYN} are the speeds calculated using the three modules described previously and which expressions are given in what follows.

2.5.1 First-order Steady-state Car-following Model

The RPA model utilizes the Van Aerde nonlinear functional form to control the steady-state behavior of traffic. The latter model was proposed by Van Aerde and Rakha (Van Aerde and Rakha 1995) and is formulated as presented in Equation 24.

$$s_{n+1}^{VA} = c_1 + \frac{c_2}{u_f - u_{n+1}} + c_3 u_{n+1} \qquad (24)$$

Here s_{n+1}^{VA} is the steady state spacing (in meters) between the leading and the following vehicles, u_{n+1} is the speed of the follower, in (m/s), u_f is the free-flow speed expressed in m/s, and c_1 (m), c_2 (m²/s) and c_3 (s) are constants used for the Van Aerde steady-state model that have been shown to be directly related to the macroscopic parameters defining the fundamental diagram of the roadway.

Finally, it should be noted that from the perspective of car-following modeling, the main objective is to determine how the following vehicle responds to changes in the behavior of the leading vehicle. Subsequently, a speed formulation is adopted for the Van Aerde model, as demonstrated in Equation 25, which is easily derived from Equation 24 using basic mathematics.

$$u_{n+1}^{VA}$$
$$= \frac{-c_1 + c_3 u_f + s_{n+1} - \sqrt{(c_1 - c_3 u_f - s_{n+1})^2 - 4c_3(s_{n+1}u_f - c_1 u_f - c_2)}}{2c_3} \qquad (25)$$

2.5.2 Collision Avoidance Model

The expression of the collision avoidance term is shown in Equation 26 and is directly related to a simple derivation of the maximum distance that a vehicle can travel to decelerate from its initial speed to the speed of the vehicle ahead of it while ensuring that, in the case of a complete stop, the jam density spacing between the two vehicles is respected.

$$u_{n+1}^{CA} = \sqrt{(u_{n+1})^2 + 2b(s_{n+1} - s_j)} \qquad (26)$$

Here b is the maximum deceleration at which the vehicles are allowed to decelerate and s_j is the spacing at jam density.

2.5.3 Vehicle Dynamics Model

The final component of the RPA model is the vehicle dynamics model (Rakha, Lucic et al. 2001, Rakha, Snare et al. 2004) that ensures that the vehicle's mechanical capabilities do not limit it from attaining the speeds that are dictated by the steady-state component. This model computes the typical acceleration of the following vehicle as the ratio of the resultant force to the vehicle mass M (Equation 27). The resultant force is computed as the difference between the tractive force acting on the following vehicle F_{n+1} (Equation 28) and the sum of the resistive forces acting on the vehicle which include the aerodynamics, rolling and grade resistances.

$$a_{n+1}^{DYN} = \frac{F_{n+1} - (0.5\rho C_d C_h A_f g u_{n+1}^2 + MgC_{r0}(C_{r1}u_{n+1} + C_{r2}) + MgG)}{M} \qquad (27)$$

$$F_{n+1} = min\left(3600\eta \frac{\gamma P}{u_{n+1}}, M_{ta}g\mu\right) \qquad (28)$$

Here η is the driveline efficiency (unitless); P is the vehicle power (kW); M_{ta} is the mass of the vehicle on the tractive axle (kg); γ is the vehicle throttle level (taken as the percentage of the maximum observed throttle level that a certain driver uses); g is the gravitational acceleration (9.8067 m/s²); μ is the coefficient of road adhesion or the coefficient of friction (unitless); ρ is the air density at sea level and a temperature of 15°C (1.2256 kg/m³); C_d is the vehicle drag coefficient (unitless), typically 0.30; C_h is the altitude correction factor equal to $1-0.000085h$, where h is the altitude in meters (unitless); A_f is the vehicle frontal area (m²), typically 0.85 multiplied by the height and width of the vehicle; C_{r0} is a rolling resistance constant that varies as a function of the pavement type and condition (unitless); C_{r1} is the second rolling resistance constant (h/km); C_{r2} is the third rolling resistance constant (unitless); m is the total vehicle mass (kg); and G is the roadway grade (unitless).

The acceleration computed using the dynamics model is then used to calculate the maximum feasible speed u_{n+1}^{DYN} using a first Euler approximation.

2.6 Fadhloun-Rakha Model

The Fadhloun-Rakha (FR) model (Fadhloun and Rakha 2019) is an acceleration-based car-following model that uses the same steady-state formulation and respects the same vehicle dynamics as the RPA model. Additionally, the model uses very similar collision-avoidance strategies to ensure a safe follow-

ing distance between vehicles.

The mathematical expression of the FR model, presented in Equation 29, estimates the acceleration of the following vehicle as the sum of two terms. The first term models the vehicle behavior in the acceleration regime, while the second governs the deceleration regime.

$$a_{n+1} = F \times a_{n+1}^{DYN} - CA(u_{n+1}, s_{n+1}, \Delta u_{n+1}) \qquad (29)$$

In the acceleration regime, the vehicle behavior is governed by the vehicle dynamics, as demonstrated in Equation 27 to ensure that vehicle accelerations are realistic. A reducing multiplier F (Equation 30), which ranges between 0.0 and 1.0, is then applied to the vehicle dynamics acceleration. The F factor is a function that is sensitive to X_{n+1} (Equation 31) which represents the ratio of u_{n+1}/s_{n+1} divided by the ratio of the steady state speed to the steady state spacing $u_{n+1}^{VA}/s_{n+1}^{VA}$. It aims to guarantee that two objectives are met. First, it ensures the convergence of the vehicles' behavior towards the Van Aerde steady state model. Second, it attempts to model human behavior and the different patterns of driving by acting as a reduction factor to the vehicle dynamics model.

$$F(X_{n+1}) = e^{-aX_{n+1}}\left(1 - X_{n+1}^b e^{b(1-X_{n+1})}\right)^d \qquad (30)$$

$$X_{n+1} = \frac{s_{n+1}^{VA}}{s_{n+1}} \cdot \frac{u_{n+1}}{u_{n+1}^{VA}} \qquad (31)$$

Where a, b, and d are model parameters that are calibrated to a specific driver and model the driver input to the gas pedal.

The second term in the expression of the FR model considers vehicle deceleration to avoid a collision with a slower traveling lead vehicle as shown in Equations (32-33). As shown, collision avoidance is ensured by the function CA which computes the needed deceleration to apply as the ratio of the square of the kinematics deceleration needed to decelerate from the current speed to the leading vehicle speed at a desired deceleration level that is set by the user.

$$d_{kinematics} = \frac{\left[u_{n+1}^2 - u_n^2 + \sqrt{(u_{n+1}^2 - u_n^2)^2}\right]}{4(s_{n+1} - s_j)} \qquad (32)$$

$$CA(u_{n+1}, s_{n+1}, \Delta u_{n+1}) = \frac{d_{kinematics}^2}{(d_{desired} - gG)} \qquad (33)$$

Where d_{des} is the desired deceleration level.

Finally, to model the effect of the driver error in estimating the leading vehicle speed and the distance gap between the two vehicles, two wiener processes are incorporated in the model formulation at the level

of u_n and s_{n+1}. Additionally, a white noise signal is added to the model's expression to capture the driver's imperfection while applying the gas pedal. The compounding effect of those three signals makes the model output more representative of human driving behavior.

3 NATURALISTIC DATASET

The data used herein represents a small subset that was extracted from the naturalistic driving database generated by the 100-Car study (Dingus, Klauer et al. 2006) that was conducted by the Virginia Tech Transportation Institute (VTTI) in 2002. In fact, VTTI initiated a study where 100 cars were instrumented and driven by a total of 108 drivers around the District of Columbia (DC) area. The resulting database from the 100-Car study (Dingus, Klauer et al. 2006) contained detailed logs of more than 207,000 completed trips with a total duration of around 20 million minutes of data.

The naturalistic dataset that was used to validate the proposed model contains information relating to 1,659 car-following events which spans over a duration of around 13 hours which is significant for the task of validation of car-following models. The car-following data composing the dataset comes from six different drivers and was collected on a relatively short segment of the Dulles Airport access road (approximately an 8-mile long section) in order to maintain facility homogeneity.

Finally, it is noteworthy to state that both the characteristics of the different vehicles are known due to the naturalistic nature of the dataset. This makes the determination of the different FR and RPA model variables straightforward and exclusive of bias.

4 PARAMETER CALIBRATION OF THE STUDIED MODELS

For each of the studied models, a certain number of inputs is needed. These inputs can be categorized into two groups. The first category comprises the inputs that are the same for the different models, namely the time-space and the time-speed profiles of the leading vehicle, the starting location and speed of the following vehicle as well as the free-flow speed (u_f) which was estimated specifically for each car-following event along with any other variables related to the roadway. The use of the free-flow speed distribution shown in Figure 1 instead of a constant value across all of the events, is justified by the

significant heterogeneity of the driver behavior during the free driving phase. In fact, drivers do not necessarily drive at the speed limit of the facility when there is no vehicle ahead of them.

Besides that, the desired speed of a certain naturalistic event was set equally across all of the studied models in order to maintain the homogeneity of driver behavior and road facility for that specific event.
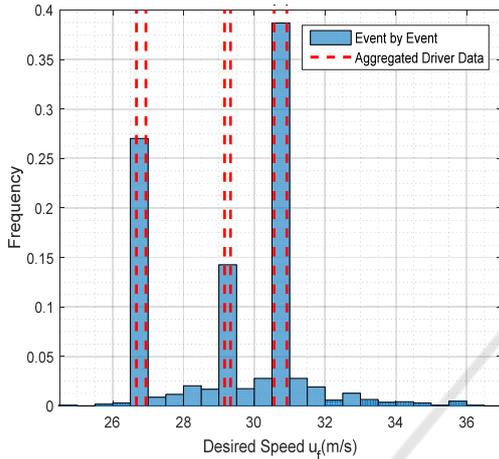

Figure 1: Distribution of the free-flow speed for the naturalistic events.

As a side remark, we note that the jam density k_j, the capacity q_c and the speed-at-capacity u_c, which are needed to generate a simulated trajectory in the case of the formulations of the RPA model and the FR model, were estimated using the calibration procedure proposed by Rakha and Arafeh (Rakha and Arafeh 2010). However, unlike the free-flow speed, those parameters were calibrated using the bulk data of each driver given their minor influence on the resulting model outputs. The estimated values for the latter driver-specific parameters are presented in Table 1a along with the needed vehicle-specific parameter values in Table 1b.

The remaining input variables consist of model-specific parameters that require to be calibrated accordingly depending on the researcher's objectives. Since this study aims to validate a new car-following model by comparing its performance to that of other state-of-the-art models, the different parameters need to be calibrated such that the resulting simulated behavior of the following vehicle matches its observed behavior as closely as possible. The calibration procedure of the different parameters of each model was conducted heuristically taking the speed RMSE as the error objective function. The choice to optimize each model with regards to the

speed RMSE is judged reasonable given that the optimization operation was done on an event-by-event basis. In fact, we opted to calibrate each model separately for each car-following event rather than for the dataset as a whole. Even though that exponentially increased the computation time, a more fair comparison between the results is made possible as each model was allowed to propose its best possible fit for each of the 1659 naturalistic events. Hence, the different model outputs are incorporative of the effect of the strength points of each model.

Table 1a: Values of k_j, q_c and u_c for each driver.

Driver	kj (veh/m)	qc (veh/s)	uc (m/s)
Driver_124	0.091	0.865	22.22
Driver_304	0.150	0.833	19.00
Driver_316	0.075	0.464	21.36
Driver_350	0.080	0.529	21.28
Driver_358	0.087	0.447	19.53
Driver_363	0.131	0.906	23.69

Table 1b: Characteristics of the different vehicles.

Driver	Vehicle Characteristics			
	P (kW)	M (kg)	C_d	A_f (m²)
Driver_124	90	1190	0.36	2.06
Driver_304	90	1090	0.40	2.00
Driver_316	90	1090	0.40	2.00
Driver_350	90	1090	0.40	2.00
Driver_358	145	1375	0.40	2.18
Driver_363	145	1375	0.40	2.18

Finally, given the presence of noise in the proposed model, the calibration was conducted using a bi-level procedure. First, the model parameters were calibrated deterministically without the consideration of the noise signals. Next, to model the effect of the noise, the optimized parameters of the first step were used to run a total of 1000 simulations in order to have valid model outputs and to determine the 95% confidence interval of the results.

5 RESULTS AND MODEL VALIDATION

Having access to the calibrated parameters, the speed profiles were obtained for each car-following event of the naturalistic dataset. The corresponding speed

outputs ensure a minimal RMSE between a model's predictions and the measured data over its whole timespan. To illustrate the results, the probability distribution of the speed RMSE of the different models is plotted in Figure 2. The figure demonstrates that the FR model performs better overall in terms of fitting the observed data than the other models. That is demonstrated by the fact that its RMSE distribution is higher than those of the other models towards the lower end of the speed errors (between 0 and 0.5). Then, as the RMSE keeps getting bigger and bigger, the tendency is reversed and the RMSE distribution of the FR model becomes the smallest.
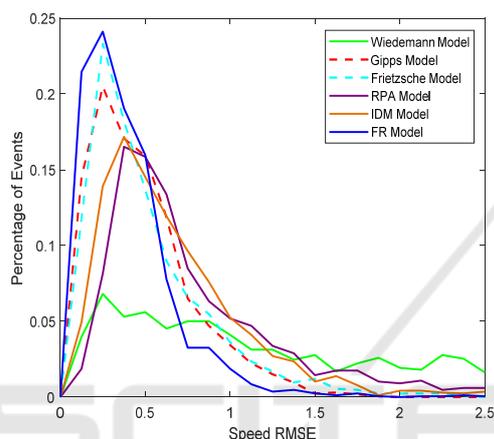

Figure 2: Probability distribution of the speed RMSE for the different models.

To better quantify statistically the difference in performance between the proposed model and the other five models, the rank of the new model was determined for each event based on the calculated RMSE value (the resulting mean of the 1000 trials). The ranking was sorted in an increasing direction of the RMSE value with the best model being the one offering the lowest error. Table 2.a shows the results of this analysis where the rank distribution of the proposed model is presented. From the table, one can see that the FR model outperformed the other ones. In fact, this model offered the best fit to the empirical data for about half of the considered events (735 out of 1659 events). Furthermore, the number of events for which the fit of the proposed model was in either the first or the second position, represents about two thirds of the total cases (1126 out of 1659 events).

The quantitative analysis was taken a step further as the proposed model was compared face-to-face with each of the studied models. That would allow for a better understanding of the new model's performance. Figure 3.a and Figure 3.b present the results of this comparison in terms of the optimized

speed RMSE and the one computed from the resulting acceleration profiles, respectively. In terms of speed error, the FR model is demonstrated to significantly outperform the other models. In fact, its speed RMSE was smaller than that found using the RPA, Gipps, Wiedemann, Frietzsche, and the IDM models in between 65% to around 90% of the events. The previous stated values do not confer enough information about the new model performance by themselves as they do not quantify the percentages by which the error function was reduced. Consequently, the bar chart of Figure 3 is complemented by Table 2.b which presents key measures (mean, median and standard deviation) about the distribution of the relative percentage decrease in the speed RMSE. For instance, it is found that for the 90% of the total events for which the proposed model formulation outperformed the Wiedemann model, the error reduction percentage had a median equal to 85%. In the case of the RPA model, the FR model resulted in an average decrease of the RMSE that is around 56% for the 88% of the events for which it was the best.
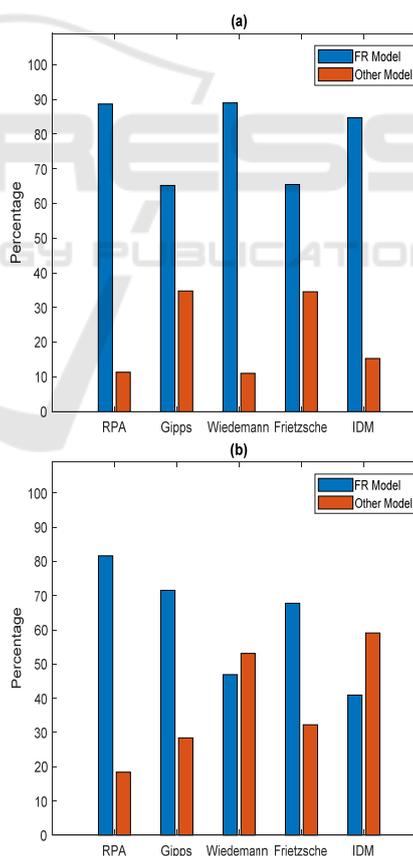

Figure 3: Comparison of the proposed FR model formulation performance to the other models: a. Based on the speed RMSE; b. Based on the acceleration RMSE.

When considering face-to-face comparisons in terms of the resulting acceleration data from the optimized speed profiles, only the Wiedemann and the IDM model outperformed the FR model as it can be observed in Figure 3.b. While the IDM model is known for its excellent fit to acceleration data due to its smooth expression, the results of the Wiedemann model seem intriguing at first. In fact, it is found that the results are justified by the structure of the Wiedemann model itself as it will be described later.

Table 2a: Rank of the FR model in terms of goodness of fit as a percentage of the total number of events using the speed RMSE.

Rank	Rank Distribution (%)
1	44.30
2	23.57
3	16.88
4	11.63
5	3.32
6	0.30

Table 2b: Distribution characteristics of the decrease percentage in the speed RMSE for head-to-head comparisons.

	Best	Mean	Median	Std Dev
RPA		56.3	58.6	23.7
G		45.4	46.9	22.4
W	FR	77.0	85.7	20.9
F		45.6	46.9	22.7
IDM		50.5	53.4	21.5
RPA	RPA	26.6	22.7	18.7
G	G	43.2	45.6	23.3
W	W	43.9	45.4	24.4
F	F	35.9	35.8	22.1
IDM	IDM	30.3	27.5	20.8

In order to examine the performance of the different models qualitatively, the resulting simulated speeds are presented for some sample events. In fact, Figure 4 plots the variation of the observed and simulated speed profiles for four different events over time. For each subplot (Figure 4a through Figure 4d), the results from the studied models are drawn in order to compare their predictions with the observed

naturalistic behavior. For example, for the event presented in Figure 4a, the driver accelerated from about 23.5 m/s to around 26 m/s, maintained his/her speed around that value, then re-accelerated to about 27 m/s and tried to maintain that speed until the end of the event. This behavior was well captured by most of the studied models, except that at the end of the event all models predicted a decrease in speed. This is mainly due to the fact that all the studied models take into account a minimum safe distance in order to avoid collision with the leading vehicle. Given that the collision avoidance logics of the models judged that the spacing maintained by the driver is unsafe for such high speeds, a decrease in speed was predicted to keep a safe distance and to ensure that the collision avoidance conditions are met. That opposes the actual driver behavior who maintained his/her driving speed despite being unsafely close to the leading vehicle. Looking roughly into this event, it is the FR model that traces better the actual driver behavior, followed by the IDM model, then Gipps, the RPA and Frietzsche models, and lastly Wiedemann model.

It is worth clarifying at this level the reasons behind the steep decrease in speed observed in the output of the Wiedemann model. The observed speed drop, which occurs 30 seconds after the start of the event, is due to the nomenclature of Wiedemann model itself. In fact, similar data cliffs were found to be present in a noticeable number of other events for this model. Such behaviors result from the abrupt change in the acceleration value when transitioning from one traffic regime to another. Besides the latter aspect, the crossing of one of the boundaries delimiting the different regions of the Wiedemann model was found to result in another disparity in the model output when compared to most of the other models (FR, RPA, Gipps, IDM). The concerned disparity is observed when the following vehicle remains in the same traffic region for the entire duration of the car-following event, hence arising the possibility of having a constant acceleration over the entire duration of the car-following maneuver. The previous two drawbacks are also manifested in the Frietzsche model due to its similar structure, however their presence is not as prevalent. For instance, one such case in which the following vehicle remained within the same traffic regime for Frietzsche model is shown in Figure 4c. The figure illustrates a scenario in which the driver was trying to maintain his/her desired speed of 28.5 m/s with minor fluctuations. Since the vehicle started and finished its trip within the "Free Driving" regime, the Frietzsche model resulted in a constant speed profile for the entire

event. However, the latter aspects of Frietzsche and Wiedemann models do not necessarily connote an inability to propose a fitted speed that matches empirical data. As a matter of fact, while all the models captured the empirical behavior of the event presented in Figure 4b, the Frietzsche model was the best in terms of tracing the actual speed profile. All other models slightly over-predicted the maximum reached speed.

Finally, concerning the event described by Figure 4d, the speed profile suggests that the highway is heavily congested. The driver decelerated from about 9 m/s to come to an almost complete stop for a few seconds. This was followed by an oscillatory behavior due to a succession of accelerations and decelerations. Despite the repeating oscillations, the FR model traced almost perfectly the driver behavior

for the entire timespan. The RPA model gave reasonable predictions for this event as well. Overall, as a qualitative measure, the different events presented in the figure are consistent with the goodness of fit results presented earlier. The Gipps model along with the FR and RPA model appear to capture the naturalistic data considerably well.

Next, the acceleration profiles derived from the calibrated speed data were examined. For illustration purposes, a sample event was chosen to visualize and compare the simulated acceleration profiles to empirical data. The different profiles are presented in Figure 5. For clarity of the figure as the overlap between the outputs of the studied models is significant, the results are presented in each sub-figure (Figure 5a through Figure 5f) along with the
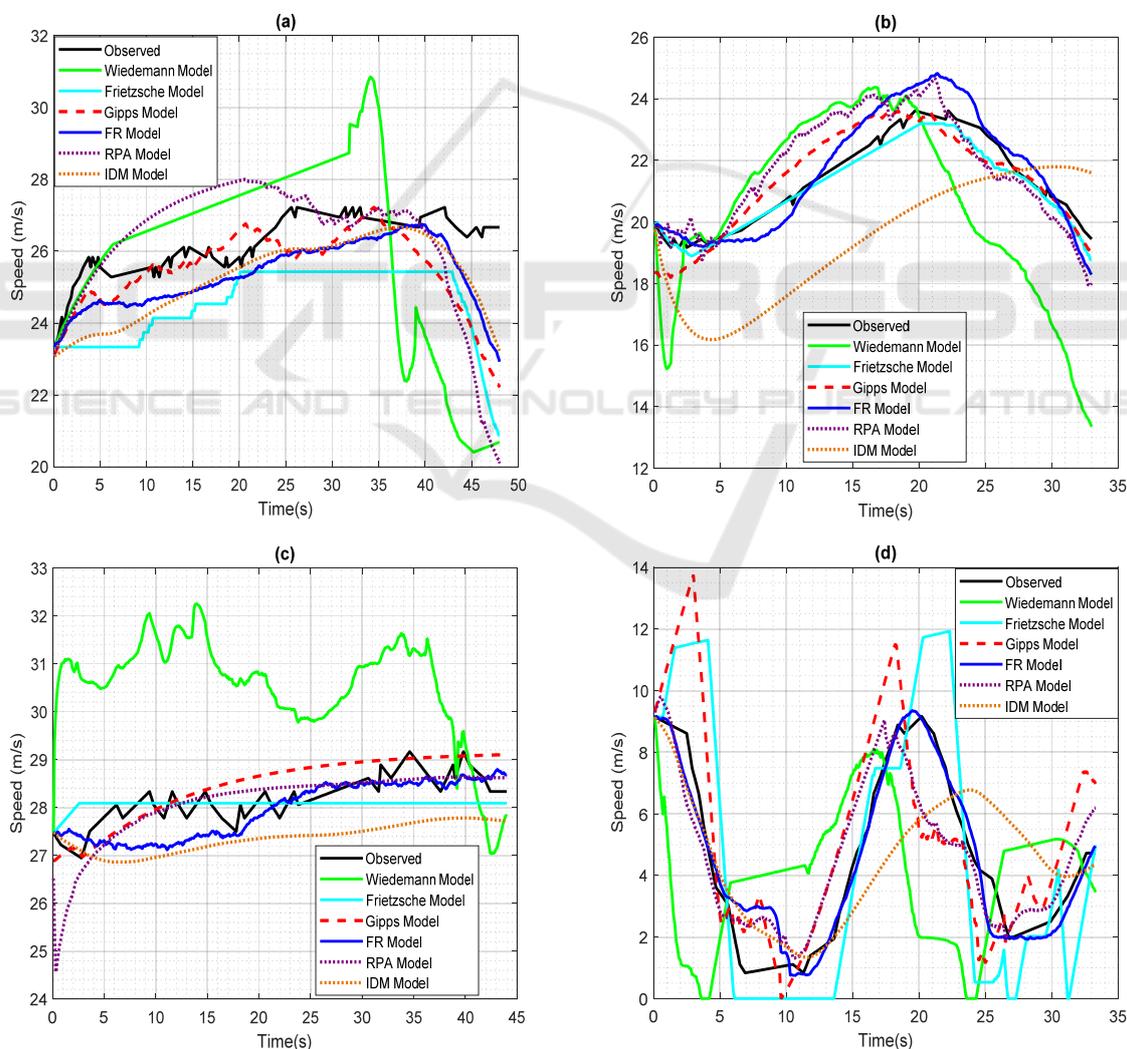

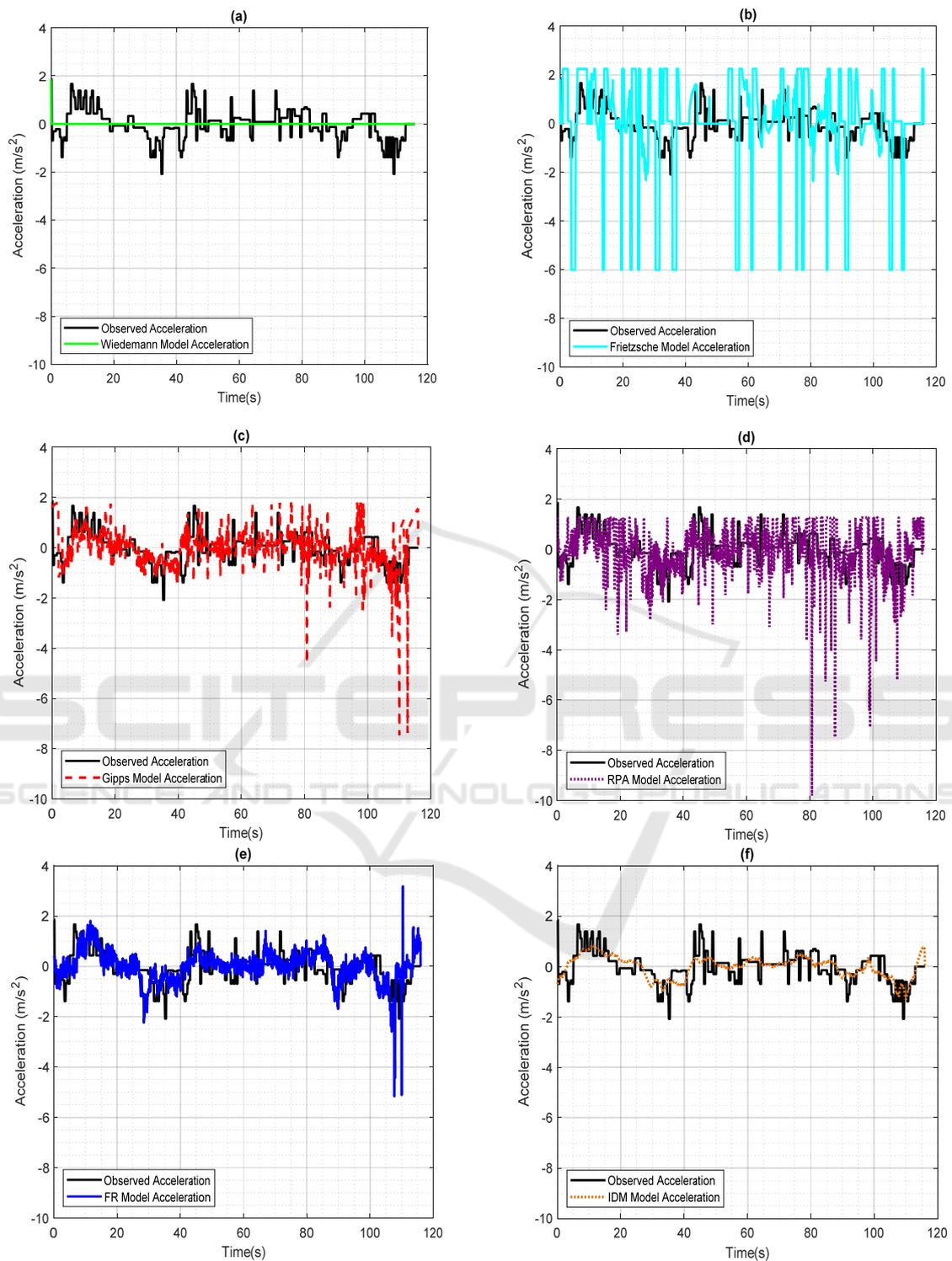Figure 4: Variation of the simulated speeds over time of four sample events.

Figure 5: Variation of the simulated acceleration over time of a sample car-following event: a. Wiedemann model; b. Frietzsche model; c. Gipps model; d. RPA model; e. FR model; f. IDM Model.

observed acceleration of the driver. During this 2-minute car-following event, the driver had

acceleration and deceleration maneuvers with maximum values of 1.6 m/s² and 2.1 m/s²,

189

respectively. As shown by Figure 5a, the Wiedemann model results in a zero constant acceleration mainly because the modeled vehicle behavior remained within the boundaries of one of the traffic regimes for the total event duration.

More importantly, the illustrated constant acceleration behavior of the Wiedemann model, which was confirmed across several other car-following events, gives a plausible explanation of the extremely low values found when the RMSEs related to the acceleration data were computed. By avoiding the oscillatory behavior of the other models and, more importantly, staying within the maximum acceleration and deceleration values without overshooting, a constant acceleration profile would result in a better fit to the empirical behavior in terms of the RMSE value. Setting aside the car-following events with a constant simulated acceleration, the Wiedemann model resulted in a stepped acceleration profile similar to the acceleration-time diagram of the Frietzsche model plotted in Figure 5b. As for Gipps model, the FR model and the RPA model (Figure 5c, Figure 5d, and Figure 5e, respectively), they resulted in acceleration values that closely followed the field data even though the maximum predicted deceleration was relatively overestimated. More precisely, the IDM model traced the actual acceleration profile the best for this specific event followed by the FR model formulation. Generally speaking, the new model was found to be the best in terms of mimicking the real driver behavior as it successfully avoided the acceleration fluctuations produced by the other models that are far in excess of those observed at the level of the empirical data. Even more, the significance and contribution of the latter finding is further amplified given the fact that the FR model formulation is inclusive of three noise signals. Those noises attempt to account for the driver's errors related to estimating the model input variables — the distance gap to the leading vehicle along with its speed — as well as his/her imperfection while applying the gas pedal. Notwithstanding the fact that the other models are exclusive of such errors giving them a statistical edge, their predicted acceleration profiles were still outperformed by the acceleration predictions of the FR model except for the IDM model which provides comparable results.

From a traffic researcher standpoint, acceleration data can be cast as the most important output of a car-following model. In fact, acceleration information is the starting point for the computation of other measures of effectiveness (MOEs). Two specific MOEs that are very sensitive to the accuracy of predicted accelerations and quite important from an environmental perspective, are fuel consumption and emissions estimations. With that in mind, it seemed necessary to examine the behavior of the maximum acceleration distribution of the bulk dataset given its major impact on any fuel consumption or emissions calculation.

Subsequently, the observed and predicted maximum acceleration of each model were extracted for each event and plotted as shown by Figure 6. We note here that the maximum acceleration data is sorted from the highest value to the lowest for each model independently of the others. This means that the event numbered as one, for example, in the figure is not the same physical event for all the studied models or that calculated from the measured speed data. It is just the physical event that resulted in the highest maximum observed or modeled acceleration. In other words, the figure does not allow making event-by-event comparisons between the different models. The main purpose of the plot is to compare the empirical maximum acceleration distribution of the whole dataset to the ones resulting from the calibration of the different studied models.

As a side note, since 1000 simulations were run using the logic of the FR model to estimate the mean and the dispersion of the results, the simulated maximum acceleration using the new model formulation is plotted using the mean and the 95% confidence interval of the data which is shown by the light bounded area in Figure 6. Qualitatively speaking, the figure demonstrate the superiority of the FR model in terms of its ability of replicating the maximum acceleration behavior of the naturalistic dataset. In fact, the observed data appears to be successfully covered by the breadth of the 95% confidence interval of the model output.
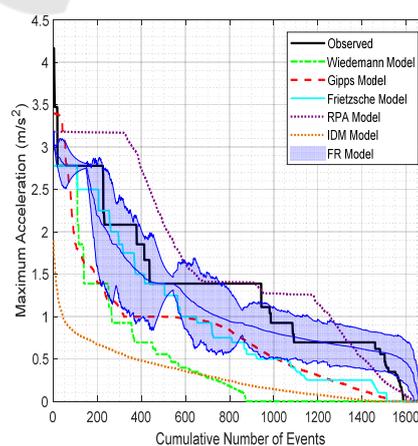

Figure 6: Comparison of the maximum acceleration behavior of the naturalistic dataset to the outputs of the different models.

6 CONCLUSIONS AND FUTURE WORK

This research effort investigates and validates the statistical performance of the FR car-following model using naturalistic driving data from the 100-Car study. The validated model is an acceleration-based alternative formulation of the RPA model. In fact, the two models share the same steady state model, respect the same vehicle dynamics and use different, but very similar, collision-avoidance strategies to ensure a safe following distance between cars.

The considered naturalistic data of six drivers was used to calibrate the FR model along with five state-of-the-art car-following models, and a comparative analysis between the resulting model performances was conducted. By doing so, this study demonstrates that the FR model outperforms Gipps, Wiedemann, Frietzsche, the RPA and the IDM models in terms of statistically matching the empirical data on an event-by-event basis.

While the RMSE, used herein, is a good indicator to evaluate a car-following model from a statistical perspective, it is not generally enough to confirm that it would be the best with regards to every aspect of traffic engineering. In fact, the only endpoint that can be deducted from this study is that the FR model is the most flexible when compared to the other ones in terms of its ability to generate a speed profile for the following vehicle that emulates empirical data such that the resulting error is at its minimum. Whether the FR model formulation would offer the best fit when considering other indicators, such as fuel consumption or emissions rates, is a completely separate problem that needs to be investigated before conclusions can be made.

ACKNOWLEDGMENTS

REFERENCES

Barceló, J. (2001). GETRAM/AIMSUN: A software environment for microscopic traffic analysis. *Proc. of the Workshop on Next Generation Models for Traffic Analysis, Monitoring and Management.*

Chandler, R. E., R. Herman and E. W. Montroll (1958). "Traffic dynamics: studies in car following." *Operations research* 6(2): 165-184.

Dingus, T. A., S. G. Klauer, V. L. Neale, A. Petersen, S. E. Lee, J. Sudweeks, M. Perez, J. Hankey, D. Ramsey and S. Gupta (2006). The 100-car naturalistic driving study, Phase II-results of the 100-car field experiment.

Drew, D. R. (1968). Traffic flow theory and control.

Fadhloun, K. and H. Rakha (2019). "A novel vehicle dynamics and human behavior car-following model: Model development and preliminary testing." *International Journal of Transportation Science and Technology*, ISSN: 2046-0430.

Fritzsche, H.-T. (1994). "A model for traffic simulation." *Traffic Engineering+ Control* 35(5): 317-321.

Gazis, D. C., R. Herman and R. W. Rothery (1961). "Nonlinear follow-the-leader models of traffic flow." *Operations research* 9(4): 545-567.

Gipps, P. G. (1981). "A behavioural car-following model for computer simulation." *Transportation Research Part B: Methodological* 15(2): 105-111.

Jiang, R., Q. Wu and Z. Zhu (2001). "Full velocity difference model for a car-following theory." *Physical Review E* 64(1): 017101.

Newell, G. F. (2002). "A simplified car-following theory: a lower order model." *Transportation Research Part B: Methodological* 36(3): 195-205.

Olstam, J. J. and A. Tapani (2004). Comparison of Car-following models.

PTV-AG (2012). VISSIM 5.40–01 User Manual. Karlsruhe, Germany.

Rakha, H. and M. Arafeh (2010). "Calibrating Steady-State Traffic Stream and Car-Following Models Using Loop Detector Data." Transportation Science 44(2): 151-168.

Rakha, H., I. Lucic, S. Demarchi, J. Setti and M. Aerde (2001). "Vehicle Dynamics Model for Predicting Maximum Truck Acceleration Levels." *Journal of Transportation Engineering* 127(5): 418-425.

Rakha, H., Pasumarthy, P., and Adjerid, S. (2009). "A Simplified Behavioral Vehicle Longitudinal Motion Model." *Transportation Letters: The International Journal of Transportation Research*, Vol. 1(2), pp. 95-110.

Rakha, H., M. Snare and F. Dion (2004). "Vehicle Dynamics Model for Estimating Maximum Light-Duty Vehicle Acceleration Levels." *Transportation Research Record: Journal of the Transportation Research Board* 1883(-1): 40-49.

Smith, M., G. Duncan and S. Druitt (1995). "PARAMICS: microscopic traffic simulation for congestion management."

Soria, I., L. Elefteriadou and A. Kondyli (2014). "Assessment of car-following models by driver type and under different traffic, weather conditions using data from an instrumented vehicle." *Simulation Modelling Practice and Theory* 40: 208-220.

Treiber, M., A. Hennecke and D. Helbing (2000). "Congested traffic states in empirical observations and

microscopic simulations." *Physical review E* 62(2): 1805.

Van Aerde, M. and H. Rakha (1995). Multivariate calibration of single regime speed-flow-density relationships [road traffic management]. *Vehicle Navigation and Information Systems Conference, 1995. Proceedings*. In conjunction with the Pacific Rim TransTech Conference. 6th International VNIS. 'A Ride into the Future'.

Van Aerde, M. and H. Rakha (2007). "INTEGRATION © Release 2.30 for Windows: User's Guide - Volume II: Advanced Model Features, " M. Van Aerde & Assoc., Ltd." (Blacksburg).

Van Aerde, M. and H. Rakha (2007). "INTEGRATION © Release 2.30 for Windows: User's Guide – Volume I: Fundamental Model Features, " M. Van Aerde & Assoc., Ltd." (Blacksburg).

Wiedemann, R. (1974). Simulation des Strassenverkehrsflusses. Karlsruhe, Germany, Schriftenreihe des Instituts für Verkehrswesen der Universität Karlsruhe.

Wiedemann, R., Reiter, U. (1992). Microscopic traffic simulation: The simulation system MISSION, background and actual state. CEC Project ICARUS (V1052), Final Report. Brussels. 2: 1-53 in Appendix A.